Non-Invasive Diagnostic Evaluation of Urinary Exosomal Let-7c Cluster Expression in Bladder Cancer Using Machine Learning Approaches

Sukhad Kural[1*], Lalit Kumar[1#*], Abhay Kumar Pathak[2*], Shweta Singh[3], Garima Jain[3], Mahima Yadav[5], Yashasvi Singh[1], Ujwal Kumar[1], Sameer Trivedi[1] , Manjari Gupta[2], Vibhav Gautam[6], Parimal Das[5]

[1]*Department of Urology, Institute of Medical Sciences, Banaras Hindu University, Varanasi, India.*
[2]*Department of Computer Science, Institute of Science, Banaras Hindu University, Varanasi, India.*
[3]*MIRNOW, BioNEST, Banaras Hindu University, Varanasi, India.*
[4]*Department of Pathology, Institute of Medical Sciences, Banaras Hindu University, Varanasi, India.*
[5]*Centre for Genetic Disorders, Institute of Science, Banaras Hindu University, Varanasi, India.*
[6] *Centre of Experimental Medicine and Surgery, Institute of Medical Sciences, Banaras Hindu University, Varanasi, India.*

*Equal Contribution first author #Correspondence - lalitkumarims@bhu.ac.in

Abstract

Background: Bladder cancer (BCa) diagnosis typically relies on invasive cystoscopy, which is effective but costly and uncomfortable. Urinary microRNAs (miRNAs), especially exosomal ones, are promising non-invasive biomarkers due to their stability in biological fluids and disease specificity. However, challenges such as population variability, methodological inconsistencies and normalization issues hinder their clinical translation, emphasizing the need for innovative approaches to enhance diagnostic performance.

Objective: To evaluate the diagnostic potential of urinary exosomal let-7c cluster (let-7c-5p, miR-99a-5p and miR-125b-5p) in BCa patients by integrating miRNA expression data with Machine Learning (ML) models.

Methods: Urine samples were collected from 66 participants, including 50 BCa patients and 16 healthy controls (HC). Exosomal miRNAs were isolated and quantified using Quantitative Real-Time-Polymerase-Chain-Reaction (qRT-PCR). Statistical analysis and hypothesis tests were conducted to explore the nature and diagnostic relevance of individual biomarkers. A logistic regression classifier was applied to evaluate both the combined and differential diagnostic capabilities of the selected biomarkers. Accuracy, precision, recall and AU-ROC scores were used to assess model performance. Bioinformatics analysis was performed to identify pathways associated with the features prioritized by the ML models, ensuring their relevance to BCa.

Results: The result revealed significant differentiation between BCa patients and HC, with miR-99a-5p ($p=0.013$, AU-ROC=0.71) and miR-125b-5p ($p=0.047$, AU-ROC=0.64) demonstrating

reliable diagnostic performance (let-7c-5p showed weaker discrimination, AU-ROC=0.65, p>0.1). The logistic regression ML model achieved an accuracy of 80.0% (AU-ROC=0.86, recall=100%) in distinguishing cancer from HC and 53.3% (AU-ROC=0.63) when applied to miRNA-only grade classification. When clinical variables were integrated with miRNA expression, performance improved to 73.3% accuracy (AU-ROC=0.61) for high-versus low-grade differentiation. Across Ta–T2, miR-99a-5p displayed relatively better separation, whereas let-7c-5p and miR-125b-5p showed weak stage-related differences. The integration of bioinformatics analysis confirmed the biological relevance of these miRNAs in BCa-related pathways, including PI3K–Akt, p53, NF-κB and RAS/MAPK signaling, with hub genes such as TP53, MYC, EGFR, and CCND1 identified, further validating the diagnostic utility of the selected biomarkers.

Conclusion: Urinary let-7c cluster miRNAs demonstrate promising diagnostic potential when analyzed with ML models, offering a non-invasive alternative to conventional methods. These findings highlight the promise of ML-based approaches alongside molecular markers for advancing clinical diagnostics in BCa.

Keywords: Bladder Cancer; Liquid Biopsy; miRNAs; Urinary Biomarkers; Urine Exosomes; Machine Learning

1. Introduction

Bladder cancer (BCa) accounts for around 3–4% of cancers in men, ranking as the fourth leading cancer in males and the ninth most common globally. Despite advances in management, it is characterized by high recurrence rates and poor prognosis in advanced stages[1]. The risk factors are diverse and include tobacco use, exposure to dyes and chemicals, chronic urinary tract infections (UTIs) and long-term bladder irritation caused by the presence of catheters or bladder stones[2,3]. Few other factors include aging, gender, genetic predisposition and conditions like chronic cystitis[4]. Painless gross hematuria is the most common symptom seen in 80-90% of patients, but only 10% of those with hematuria are diagnosed with BCa[5]. BCa is a heterogeneous disease, with more than 90% of cases arising as urothelial carcinoma. Less common histological variants include squamous cell carcinoma, adenocarcinoma and neuroendocrine tumors[6]. Based on the extent of muscle invasion, BCa is categorized as non–muscle invasive BCa (NMIBCa; stages Ta, T1, CIS) or muscle-invasive BCa (MIBCa; stage T2 and above)[7]. Approximately 75% of cases are non-muscle invasive and are primarily managed with transurethral resection of bladder tumor (TURBT), chemotherapy and intravesical Bacillus Calmette-Guérin (BCG) therapy that contribute to favorable therapeutic results[8,9]. However, MIBC is typically treated with a combination of radical cystectomy (removal of the bladder) and systemic chemotherapy (including cisplatin-based regimens), sometimes followed by adjuvant therapy[10]. Although cystoscopy and urinary cytology remain the gold standards for BCa diagnosis, the invasive nature of cystoscopy and the limited sensitivity of cytology in low-grade (LG) tumors pose significant challenges[11]. As a result, both methods often fail to detect malignancies at an early stage, when treatment is most effective. Moreover, these approaches provide little information about the molecular characteristics of tumors, which are increasingly relevant for guiding therapy, underscoring the need for more effective non-invasive alternatives.

Extracellular vesicles (EVs) are a group of membrane-bound vesicles secreted by all eukaryotic cells and found in a variety of biofluids, including urine, functioning as molecular cargo carrying diverse biomolecules such as mRNAs, microRNAs (miRNAs), lncRNAs and proteins, making them great

source of biomarkers[12]. Exosomes are a subtype of EVs between 30 and 150 nm in size derived from endosomes that transfer biomolecules to facilitate cell communication and play a role in cancer progression and metastasis[13]. miRNAs are remarkably stable in adverse conditions, such as acidic or alkaline pH, thermal stress and RNase activity[14]. When enclosed in urinary exosomes, they offer a non-invasive and accessible approach for detecting and monitoring BCa, with strong clinical potential. Approximately 99.96% of urinary exosomes are released by cells from the kidney, urinary tract lining and male urogenital tract[15]. This direct exosome shedding by urological tumors into the urine makes them highly promising candidates for sensitive and urological cancer biomarkers[16].

Liquid biopsy has emerged as an effective tool for early screening, detection of tumors and for monitoring disease progression. Over the last decade, miRNAs have emerged as promising candidate for liquid biopsy based diagnostics due to their stability in biofluids, tissue specificity and key regulatory roles in cancer-associated pathways[17]. miRNAs are short, ~22-nucleotide, noncoding RNAs that modulate gene expression after transcription by binding to the 3′ untranslated regions (3′ UTRs) of target mRNAs, leading to repression of translation or mRNA degradation[18]. Gene expression is largely influenced by miRNAs and their imbalance is frequently observed in cancer[19]. Some miRNAs promote tumor development when overexpressed by suppressing genes that inhibit growth (e.g., miR-21, which targets PTEN and PDCD4 to enhance cell proliferation and survival in urologic cancers, including BCa[20]; miR-155, which inhibits DMTF1, contributing to BCa progression[21]), while others that act as tumor suppressors are often downregulated and allow cancer cells to proliferate unchecked (e.g., the let-7 family, whose reduction leads to RAS overexpression and promotes tumorigenesis in BCa[22]).

The let-7 family of miRNAs is known for its tumor-suppressive role and is significantly involved in regulating the cell cycle, differentiation and apoptosis[23]. As a tumor suppressor miRNA, let-7c is well known to regulate oncogenes such as HMGA2[24], H-Ras[25] and c-MYC[26], thereby contributing to suppression of tumor progression[27]. The let-7c/miR-99a/miR-125b cluster, located on chromosome 21, is a well-conserved group of miRNAs known for their tumor-suppressive functions across a range

of cancers[28], including BCa, hepatocellular carcinoma, prostate cancer, cholangiocarcinoma, mesothelioma and other malignancies. These miRNAs collectively target multiple cancer pathways such as mTOR, IGF1R and STAT3 modulating key processes like proliferation, apoptosis and cellular stemness[28–30]. In BCa, these miRNAs are typically downregulated in tumor tissues, which is consistent with their role in inhibiting cancer progression[31,32]. Given their ability to regulate multiple oncogenic pathways and the strength of existing evidence, the let-7c cluster was selected for analysis in BCa as a potential non-invasive biomarker for diagnosis and monitoring disease progression.

Machine Learning (ML), a branch of Artificial Intelligence (AI), enables systems to learn from data without being explicitly programmed. Instead of relying on explicit coding, ML models leverage algorithms to uncover patterns in data, which enables predictive and decision-making capabilities. Supervised, unsupervised, semi-supervised, and reinforcement learning form the four categories of ML models, each fulfilling different functions[33]. As these models process more data, they improve over time, making ML a powerful tool across many domains, including healthcare[34,35].

In biological research, ML is revolutionizing the way we analyze complex datasets such as genomics, proteomics and medical imaging[36]. Deep biological datasets like sequencing are often large, noisy, and nonlinear, which is where ML shines. For example, ML has been widely used in cancer diagnostics, particularly in biomarker discovery, by analyzing RNA sequencing or microarray data[37]. However, despite its successes, supervised learning models especially in analyzing Quantitative Real-Time Polymerase Chain Reaction (qRT-PCR) data are still underutilized. Few studies have effectively leveraged qRT-PCR data with supervised learning to improve diagnostic accuracy[38]. This study presents one of very few studies with integrative demonstration of supervised ML applied directly to qRT-PCR derived profiling in cancer, highlighting a clinically scalable and cost-effective approach that advances the translational potential of liquid biopsy diagnostics.

Linear regression, which assumes a straight forward relationship between inputs and outputs, is frequently used but has its limitations[39]. Logistic regression, in contrast, is a widely used supervised model that performs effectively on binary classification tasks, such as identifying diseased versus

healthy conditions[40]. This algorithm estimates the probability of a binary outcome using a logistic function, making it ideal for analyzing diagnostic data like qRT-PCR results[41]. While logistic regression is simple, it can be very powerful when combined with proper feature selection and normalization. Additionally, its interpretability makes it valuable in biological research, where understanding the significance of each feature is essential.

To strengthen these findings, we conducted bioinformatics analyses including target prediction, overlap with BCa-specific genes, functional enrichment and PPI network construction. These analyses demonstrated that the dysregulated miRNAs identified in our cohort are linked to established pathways of BCa progression, thereby reinforcing their biological relevance. By integrating experimental data with in silico validation, our study provides supportive evidence for the development of a non-invasive, exosome-based diagnostic framework for BCa.

1.1. Research Gap

Even though research on BCa has advanced significantly, non-invasive diagnostic techniques have not been widely adopted as alternatives to invasive procedures in clinical settings and their current application is still primarily complementary rather than independent. For example, a number of urine-based tests that have received U.S. Food and Drug Administration (FDA) approval, including Nuclear Matrix Protein 22 (NMP22) BladderChek, Bladder Tumor Antigen (BTA) stat and UroVysion Fluorescence In Situ Hybridization (FISH), which proves potential and clinical relevance of non-invasive testing[42]. However, these tests have drawbacks, such as NMP22 and BTA stat shows high false positives in the presence of hematuria (blood in urine) or inflammation, while UroVysion FISH, though more effective in HG disease, performs poorly in LG cases and is also costly and technically demanding, which has limited their use to supportive tests rather than replacements for cystoscopy, with urine cytology often used as a complementary test[43]. Although there are few studies which investigated the let-7c cluster in BCa[32,44], not enough is known about its diagnostic aspect in urinary exosomes. Moreover, there has been limited study of qRT-PCR derived miRNA expression data examined using supervised ML models in the current literature, which has concentrated chiefly

on high-throughput platforms like microarrays and RNA sequencing for biomarker discovery[38,45]. In this study, we explored the potential of applying supervised ML to qRT-PCR derived urinary exosomal miRNA data, an approach being more practical and accessible than sequencing-based platforms. Incorporating ML offers the ability to capture subtle fluctuations in expression features that conventional linear statistical methods may overlook, thereby enhancing the diagnostic value of this widely used technique.

1.2. Research Questions

This study examines the urinary exosomal miRNAs, particularly the let-7c cluster as non-invasive biomarkers for BCa by combining molecular diagnostics, bioinformatics and ML. The following research questions guided the investigation:

- Assess whether let-7c cluster members (let-7c-5p, miR-99a-5p, miR-125b-5p) are differentially expressed in BCa patients compared with healthy controls (HC), as well as across different tumor grades and stages.
- Determine the diagnostic performance of qRT-PCR derived miRNA expression data using supervised ML models.
- Explore associations between miRNA expression and clinical or lifestyle variables such as tumor grade, stage, size, and tobacco use.
- Elucidate the biological pathways and molecular targets linked to these miRNAs through integrative bioinformatics analyses (PPI networks, GO/KEGG enrichment).

The purpose of raising such questions is to integrate classical biomarker discovery methods with advanced ML approaches through the development of an affordable and accessible diagnostic model for BCa. By utilizing exosomal miRNA expression, this study aims to facilitate the development of precision-based, non-invasive diagnostics with clinical relevance.

2. Methods

2.1. Study design

This prospective cohort study, involving 50 patients with BCa and 16 HC, was performed at the Department of Urology in association with the Departments of Radiology, Pathology, and the Centre for Genetic Disorders. The study was conducted following approval from the Institutional Ethics Committee (EC/3411), with written informed consent obtained from all enrolled participants. A total of 50 patients (≥18 years old) suspected of having bladder tumors who underwent primary TURBT were enrolled between October 2022 and April 2024. 16 healthy, age and sex-matched control subjects with no known urological pathology were recruited for comparative analysis of urinary let-7c cluster expression. Exclusion criteria included tumors arising in bladder diverticula, incomplete medical documentation, history of TURBT, prior chemoradiotherapy, impaired renal function and earlier pelvic malignancy. Patients who did not consent for the study were also excluded.

2.2. Sample Collection and Exosomal RNA Isolation

Approximately 25–30 mL of midstream early-morning urine was collected pre-operatively from patients undergoing TURBT using sterile urine collection vials. Samples were transferred to the laboratory within two hours of collection in a temperature-maintained (4 °C) insulated box, without any intermediate storage or freezing. A volume of 10 mL from each sample was utilized for exosomal RNA extraction using the Norgen Urine Exosome RNA Isolation Kit (Cat#47200, Norgen Biotek Corporation), following the manufacturer's protocol. A total of 20 µL of Elution Solution A (kit-provided) was used to elute RNA, whose concentration and purity were measured with a NanoDrop OneC UV-Vis Spectrophotometer (Thermo Fisher Scientific, USA) before being stored at −80 °C for downstream analyses.

2.3. Complementary DNA (cDNA) synthesis and qRT-PCR for Exosomal miRNA

Using the RevertAid First Strand cDNA Synthesis Kit (Thermo Scientific, Catalog #K1622, USA), complementary DNA (cDNA) synthesis of exosomal RNA was performed. Custom stem-loop primers were introduced to the reverse transcription reaction in order to attain specificity against miRNA

targets. **Table 1** summarizes the full set of primer sequences utilized in the study. qRT-PCR experiments were performed on the QuantStudio 6 Flex Real-Time PCR System (Applied Biosystems/Thermo Scientific, USA). 1 µL of diluted 1:5 cDNA, 6.25 µL of Maxima SYBR Green/ROX qPCR Master Mix (2X; Catalog #K0221, Thermo Scientific, USA), 1 µL of each forward and reverse primer (10 µM) and nuclease-free water for the final volume were all included in each 12.5 µL reaction. The thermal cycling technique included a 10 minute denaturation stage at 95°C, followed by 40 amplification cycles of 15 seconds at 95°C and 1 minute at 60°C. The overall experimental workflow is illustrated in **Figure 1A**.

No.	Oligo Name	Sequence (5′ → 3′)	Length (nt)
1	hsa-let-7c-5p-SL	GTCGTATCCAGTGCAGGGTCCGAGGTATTCGCACTGGATACGACAACCAT	50
2	hsa-let-7c-5p-FWQ	AACACGCTGAGGTAGTAGGTT	21
3	hsa-miR-99a-5p-SL	GTCGTATCCAGTGCAGGGTCCGAGGTATTCGCACTGGATACGACCACAAG	50
4	hsa-miR-99a-5p-FWQ	AACCGGAACCCGTAGATCC	19
5	hsa-miR-125b-5p-SL	GTCGTATCCAGTGCAGGGTCCGAGGTATTCGCACTGGATACGACTCACAA	50
6	hsa-miR-125b-5p-FWQ	AAGCACTCCCTGAGACCCTA	20
7	UniversalRevQ	TCCAGTGCAGGGTCCGAGGTA	21

Table 1: Primer Sequences Used for miRNA Reverse Transcription and qRT-PCR. (**Note:** All primers were desalted and synthesized without modifications. SL-Stem-loop primer; FWQ-Forward primer for qRT-PCR; UniversalRevQ-Universal reverse primer; hsa-Homo sapiens; nt-Nucleotides.)

A

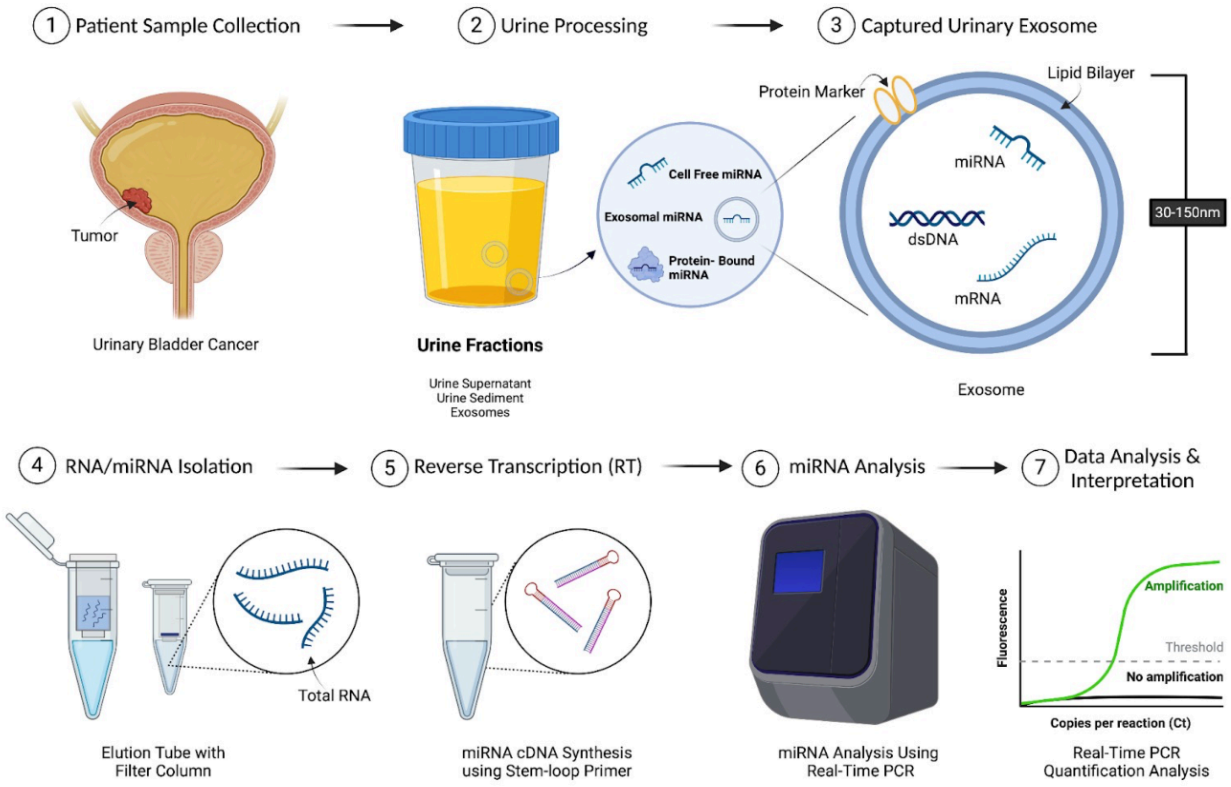

B

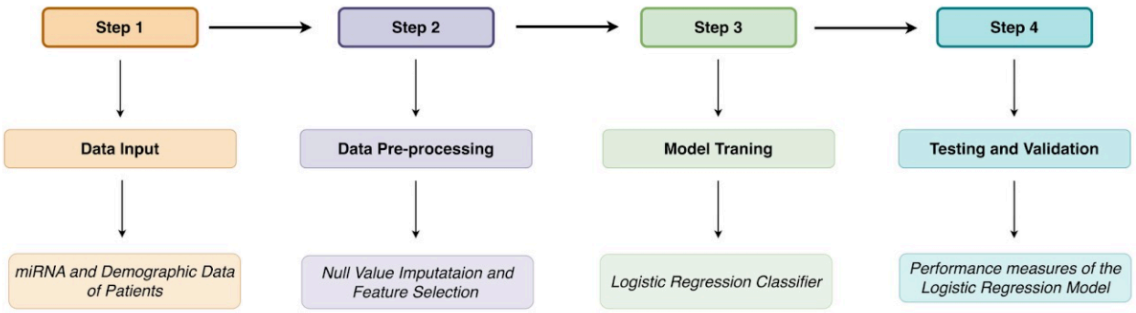

Figure 1: A. Experimental workflow illustrating the methodology used for urinary exosomal miRNA profiling in BCa. **B.** Flowchart of the model developed (Various Classification ML)

2.4. Statistical analysis

Data Preprocessing: During the preprocessing phase, we identified and handled NULL values by replacing them with the median value in the qRT-PCR derived urinary exosomal miRNA expression data . All these operations were performed on the Ct values to ensure data consistency and readiness for analysis.

Statistical Analysis: We utilized the Mann-Whitney U test, a nonparametric approach, to evaluate the hypothesis. This test is beneficial since it does not rely on a normal distribution, making it versatile and effective for assessing differences between two independent groups. We used the ROC (Receiver Operating Characteristic) curve to assess the prediction potential of different characteristics in identifying HC and BCa classes. The ROC curve is a graphical tool for determining how well a binary model works at various threshold levels. The model's performance at different threshold settings is plotted using two critical metrics: True Positive Rate (TPR) and False Positive Rate (FPR). The AUC (Area Under the Curve), which depicts the area below the ROC curve, is used to assess the model's overall ability to correctly identify and discriminate between HC and BCa.

2.5. ML-Model Development

In this study, the Logistic Regression ML model has been employed as a baseline classifier for classifying BCa from HC, and also differentiating HG and LG cancer patients in BCa using demographic and qRT-PCR dataset to capture hidden and complex patterns. The model does not utilise any hyperparameter tuning for the classification task which further ensures the reproducibility of the proposed model. We have utilised the default hyperparameter values from scikit-learn library. To assess the models predictive performance we have utilized some performance matrix such as accuracy: Accuracy measures the overall correctness of a model. It is the fraction of all predictions (both positive and negative) that the model got right; precision: Precision focuses on the quality of positive predictions. It tells us, out of all the samples the model labeled as positive, how many were actually positive. High precision means fewer false alarms; recall: Recall focuses on the completeness

of positive detection. It tells us, out of all the actual positive samples, how many the model successfully identified; F1 score: It is the harmonic mean of precision and recall. It balances the two, giving a single measure that is useful when both false positives and false negatives are important. Detailed steps of the model development process have been described in **Figure 1B**.

2.6. Bioinformatics Analysis

The target genes of 3 miRNAs were predicted using mirTarbase and Mirbase database. By removing duplicate entries all target genes list were merged, named as target gene panel (TGP) of miRNAs. Moreover, a panel of Bladder Cancer-specific genes (BCSG) panel were prepared using GeneCards, KEGG and STRING databases. The BCSG and TGP panels were crossed to identify common target genes (CTG) with Venny 2.0 (https://bioinfogp.cnb.csic.es/tools/venny/index2.0.2.html). These CTG represent the list of genes that have crucial roles in BCa molecular regulation and are regulated by let-7c cluster miRNAs. These were further explored for enrichment analysis, protein–protein interaction network construction, and pathway analysis to understand their roles in disease mechanisms. ShinyGO software was used for functional analysis of CTG panel. Cytoscape software was used for visualization and further analysis, allowing for hub genes extraction based on their crucial roles in the network.

3. Results

To evaluate the diagnostic potential of exosome-derived urinary miRNAs from the let-7c cluster in BCa, we analyzed their expression profiles using qRT-PCR in a well-characterized cohort. The study cohort consisted of BCa patients (n = 50) irrespective of tumor grade, age and sex-matched HC individuals (n = 16). The BCa cohort consisted of both HG (N=36) and LG (N=14) groups. Additionally, the BCa cohort was categorized by tumor stage into T1 (n = 32), T2 (n = 12) and Ta (n = 6). Their clinical and pathological features are summarized in **Table 2**.

Biological Sample	***Urine***	
Variable	**BCa (n=50)**	**HC (n=16)**
Age (years, mean ± SD)	59.1 ± 14.3	46.1 ± 15.0
Gender	Male: 40 (80%) Female: 10 (20%)	Male: 14 (87.5%) Female: 2 (12.5%)
Stage	Ta: 6 (12%) T1: 32 (64%) T2: 12 (24%) Carcinoma in situ: 0 (0%)	–
Grade	HG: 36 (72%) LG: 14 (28%)	–
Tumor size	Mean: 4.41 ± 2.01 >3 cm: 34 (68%) ≤3 cm: 16 (32%)	–
Number of tumors	Single: 37 (74%) Multiple: 13 (26%)	–
VI-RADS group	Low (1–3): 20 (40%) High (4–5): 30 (60%)	–
Tobacco addiction	Yes: 31 (62%) No: 19 (38%)	0 (0%)
Alcohol intake	Yes: 12 (24%) No: 38 (76%)	0 (0%)
Diabetes mellitus	Yes: 10 (20%) No: 40 (80%)	0 (0%)
Hypertension	Yes: 8 (16%) No: 42 (84%)	0 (0%)

Table 2: Clinical and general characteristics of BCa patients and HC.

3.1. Let7-c cluster gene expression pattern and correlation in BCa vs. HC

As shown in **Figure 2**, BCa patients exhibited a trend toward differential regulation of urinary exosomal let-7c-5p, miR-99a-5p and miR-125b-5p compared to HC. let-7c-5p expression was downregulated in BCa patients (P = 0.07621), miR-99a-5p and miR-125b-5p were also downregulated in BCa patients (P = 0.01327 and P = 0.08667, respectively). These results indicate that members of the let-7c cluster show a consistent trend of reduced expression in BCa relative to HC.

Urinary exosomes from both cohorts were analyzed for the expression of let7-c cluster genes or miRNA using qRT-PCR. The heatmap was created using absolute Ct values obtained that show correlation between two cohorts **(Figure 3)**. Pearson correlation analysis was used to assess relationships among urinary let-7c-5p, miR-99a-5p and miR-125b-5p in HC (Variant 0) and BCa patients (Variant 1). In HC, miR-99a-5p and miR-125b-5p showed a strong positive correlation (r = 0.73), suggesting possible co-regulation. In contrast, let-7c-5p displayed minimal correlation with either miR-99a-5p or miR-125b-5p, consistent with an independent expression pattern. Among cancer patients, correlations were weaker overall: miR-99a-5p and miR-125b-5p retained a moderate positive association (r = 0.54), while let-7c-5p shifted to weakly positive correlations with both miR-99a-5p (r = 0.37) and miR-125b-5p (r = 0.22). This attenuation of correlation in disease samples may reflect disruption of normal regulatory interactions within the let-7c cluster.

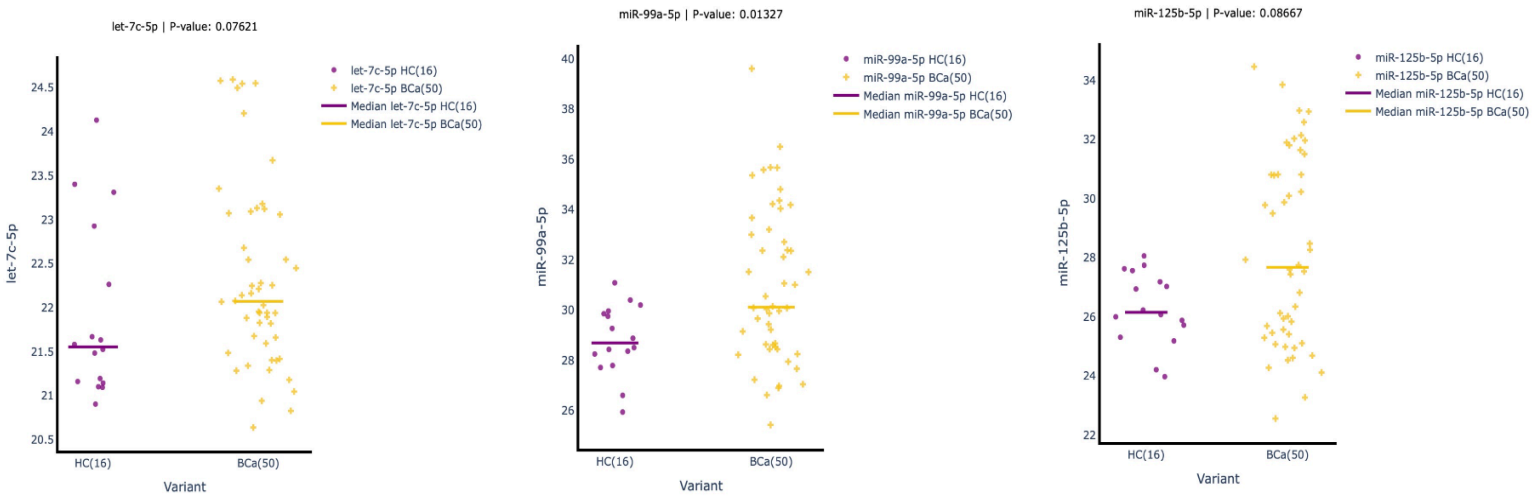

Figure 2: Expression levels of Let-7c cluster in urinary exosomes from HC (n=16) and BCa patients (n=50). Each dot represents an individual sample and horizontal lines indicate median values for each group.

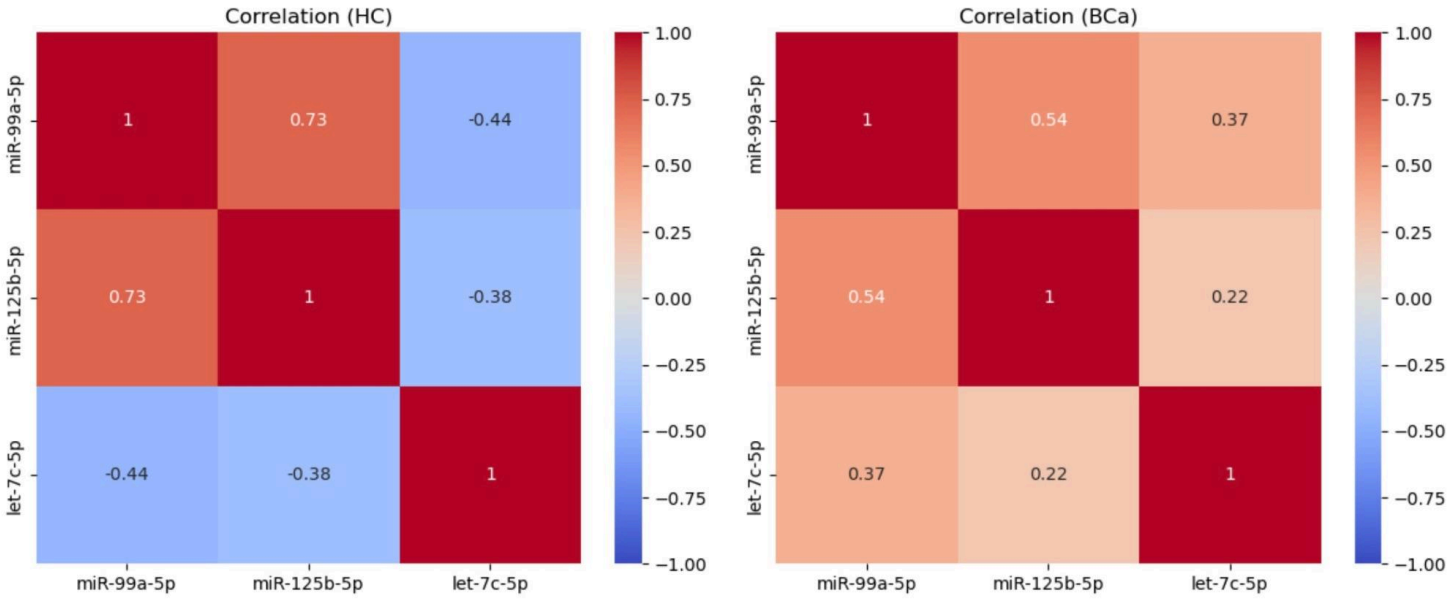

Figure 3: Correlation heatmaps of urinary miRNAs (let-7c-5p, miR-99a-5p, miR-125b-5p) in 'HC' and 'BCa' groups. Stronger positive correlations are seen in 'HCs', while 'PCa' shows weaker, more uniform positive associations, suggesting context-dependent miRNA co-regulation.

To demonstrate the discriminative power of individual urinary miRNAs in distinguishing BCa patients from HC, AU-ROC analysis was performed **(Figure 4A)**. Among these three features, miR-99a-5p exhibited the highest diagnostic accuracy with an AU-ROC of 0.71, followed by let-7c-5p (AU-ROC = 0.65) and miR-125b-5p (AU-ROC = 0.64). In addition, the diagnostic potential of the ratio of these miRNAs (such as miR-99a-5p / let-7c-5p: AU-ROC=0.32; miR-125b-5p / let-7c-5p: AU-ROC=0.64; and miR-99a-5p / mir-125b-5p: AU-ROC=0.58;) were also evaluated using AU-ROC to explore combinatorial diagnostic strength.

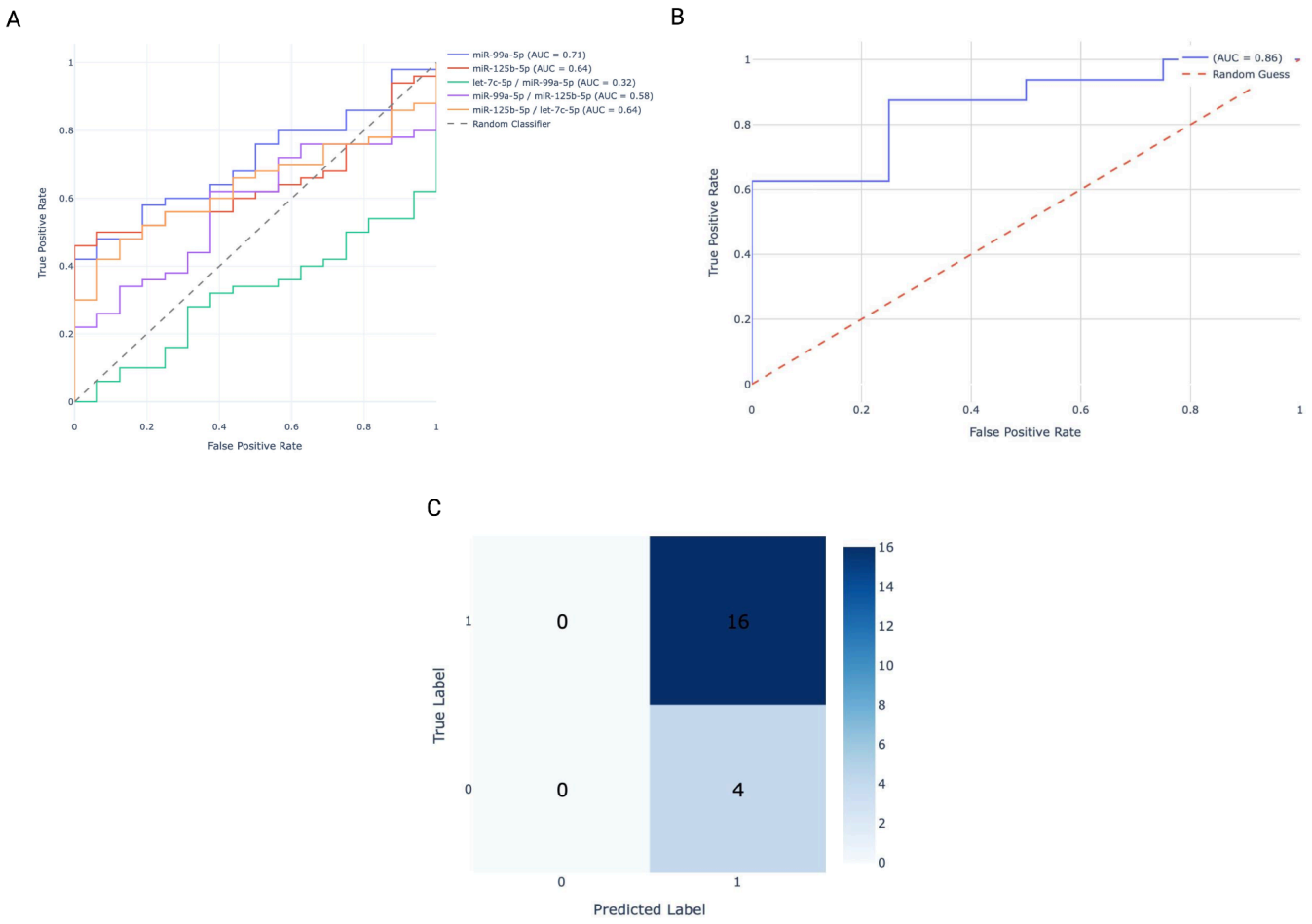

Figure 4. (A) ROC graph of individual features, **(B)** ROC graph of Logistic Regression model (HC vs BCa classification), **(C)** confusion matrix for the HC vs BCa classification.

To explore the scope of ML in this analysis, we employed logistic regression - a ML based approach. The cohort was divided into training (70%) and testing (30%) multiple features including individual miRNA: let-7c-5p, miR-99a-5p, miR-125b-5p; and ratio based features: miR-99a-5p_miR-125b-5p, miR-125b-5p_let-7c-5p and let-7c-5p_miR-99a-5p were used. The model achieved an AU-ROC of 0.86, indicating improved discriminative power as compared to individual features. The curve **Figure (4B)** shows a steep ascent towards the top-left quadrant, reflecting a high true positive rate (sensitivity) with minimal false positive classifications. The model achieved an accuracy of 80%, indicating it correctly classified 80% of the samples. With a precision (explain precision here) of 80% and a recall of 100%, it identified all true positive cases without missing any of it **Figure 4(C)** . The F1-score of 0.889 reflects a good balance between precision and recall. The confusion matrix shows no false negatives but includes some false positives.

3.2. Comparison Based on Tumor Grades (HG vs. LG)

Using the same approach, we applied a logistic regression model to distinguish HG, n=36 from LG, n=14 cases with a 70/30 training–testing split. The model achieved an accuracy of 53.3% and an AU-ROC of 0.63, indicating only modest discriminatory power, close to random classification. To investigate why the model underperformed, especially in the context of tumor grades, we next evaluated whether miRNA expression patterns were influenced by clinical and lifestyle variables that could contribute additional discriminatory value. **Table 3** reports the p-value using two different tests (t-test and Chi-square test) which are between the tumour grade and all the clinical and miRNA features.

Variable	P-value (t-test)	P-value (Chi-square test)
Age	0.182420	-
Gender	-	1.000000
Stage	-	**0.009638**
Tumor Size	0.077179	-
Number of Tumor	1.000000	-
VI-RADS Group	-	**0.000069**
Tobacco Addiction	-	0.443849
Alcohol Intake	-	0.525922
Diabetes mellitus	-	1.000000
Hypertension	-	0.279016
miR-99a-5p	0.890563	-
miR-125b-5p	0.931286	-
let-7c-5p	0.351775	-

Table 3: Hypothesis test result between Grade of cancer and all clinical variables and biomarkers.

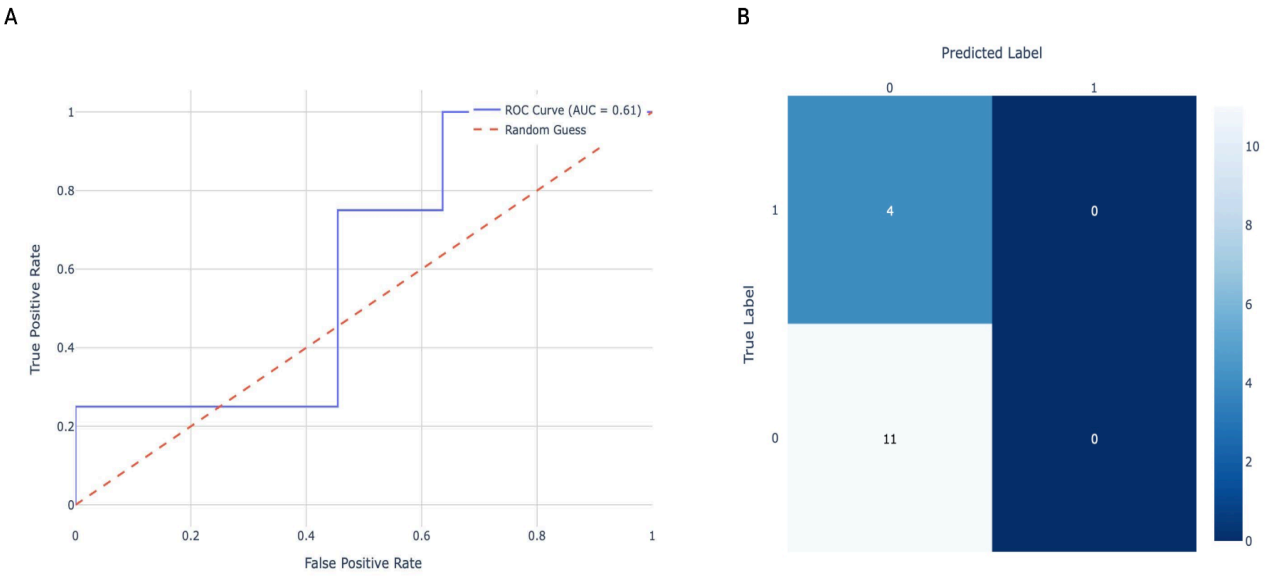

Figure 5: Results of Logistic Regression Model including molecular and clinical features as well to differentiate between HG and LG Cancer Patients. **(A)** ROC **(B)** Confusion Matrix

In the ML model, when miRNA data was combined with other clinical features showed the possibility of a potential improvement in the overall performance while distinguishing tumour grade. AU-ROC **(Figure 5A)** of 0.61 in classifying HG versus LG BCa cases using a combined feature set consisting of urinary miRNA expression (let-7c-5p, miR-99a-5p and miR-125b-5p) alongside key clinical and other variables. ML model was improved by 20% demonstrating accuracy of 73.33% presented in the confusion matrix **(Figure 5B).** However, the model achieved an AU-ROC of 0.61, indicating only modest discriminatory ability between HG and LG subgroups. While the AU-ROC curve slightly deviates from the diagonal line (0.50), the relatively flat slope and lower sensitivity values suggest that the current combination of features lack sufficient predictive power for reliable tumor grade differentiation.

3.3. Let7c cluster expression pattern in Tumor Stages (Ta, T1, T2)

Let-7c-5p showed little stage-related variation and poor classification (AU-ROC 0.32–0.36) (**Figure 6A,B**), while miR-125b-5p also demonstrated limited stage-specific value (AU-ROC 0.43–0.64). In contrast, miR-99a-5p displayed clearer differences, especially at Ta and achieved stronger discriminatory potential (AU-ROC 0.79). These findings position miR-99a-5p as the most promising of the three markers for stage evaluation, though validation in larger cohorts will be required.

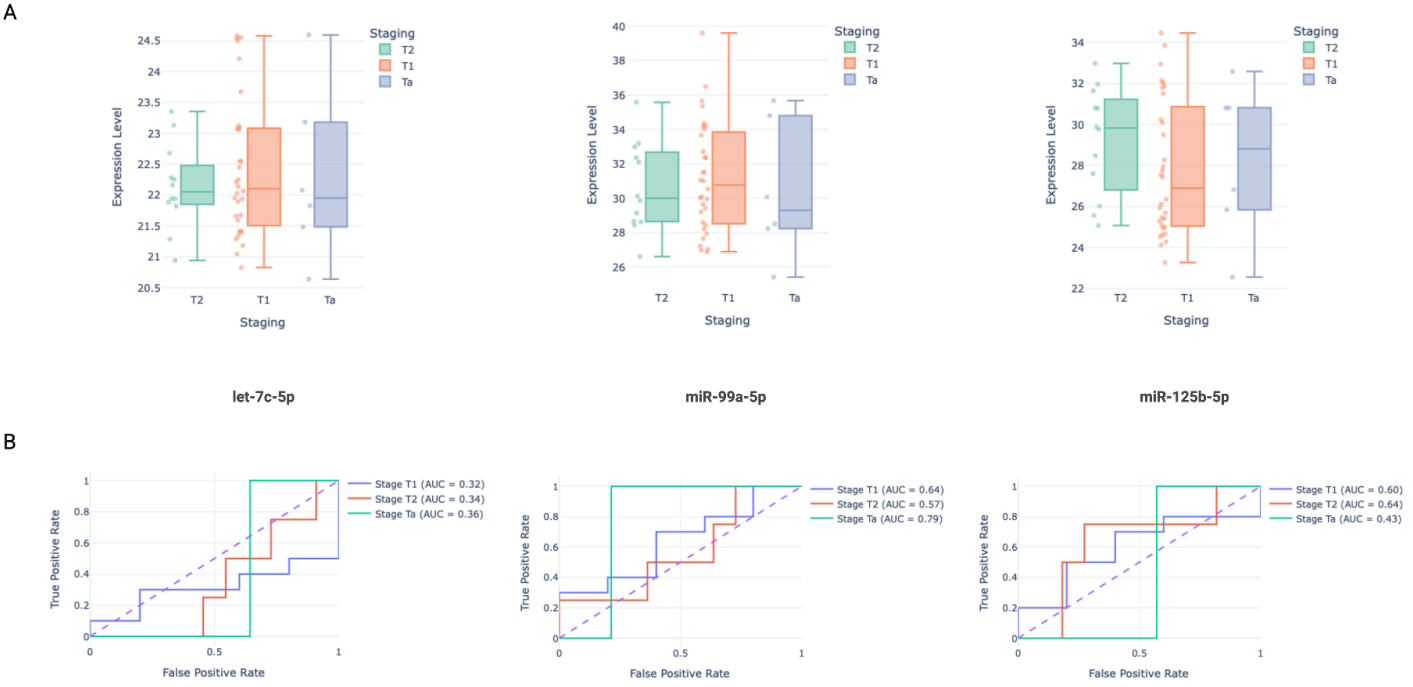

Figure 6: Boxplot and ROC of stage-specific classification: **(A)** Boxplot **(B)** ROC.

3.4. Validation of results in Bioinformatics Analysis:

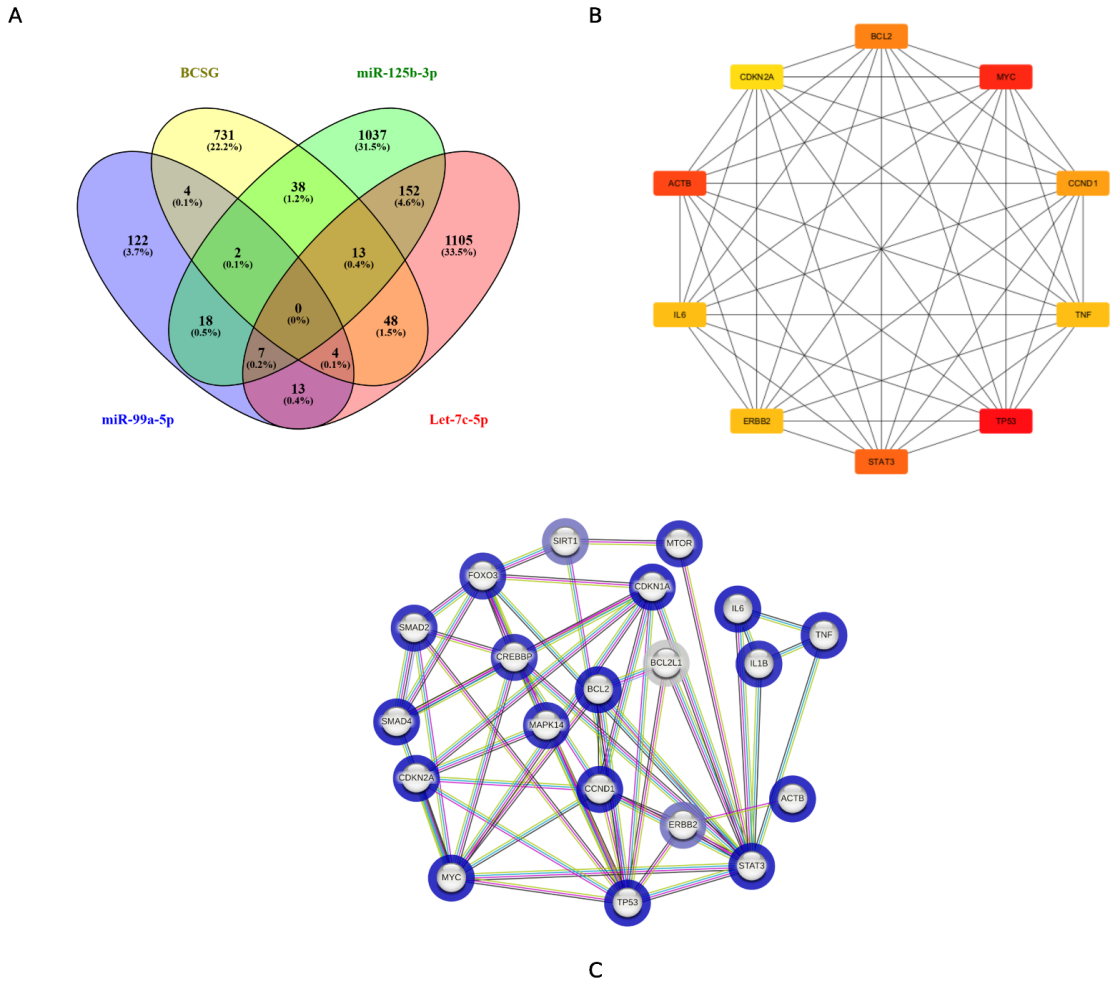

Figure 7: (A) Venn diagram showing miRNA and their target genes; common genes between the BCGS panel and miRNA gene targets were highlighted, **(B)** Top 10 genes with the highest degree scores were selected using CytoHubba tools, **(C)** miRNA–target genes and hub genes were reanalyzed using the STRING database,shown as a combined visualization.

We identified target genes of all 3 miRNAs (Let-7c-5p ,miR-99a-5p and miR-125b-5P) and predicted 3072 target genes (TGP) using mirTarbase[46] and Mirbase database[47]. The segregation of target genes of miRNAs and BCSG panel are shown in **Figure 7A.** Further, TGP and BCSG panels were crossed and 109 CTG genes that were common in both panels were selected for further analysis. The PPI network was created using CTG genes in the STRING database. To identify interaction between the target genes of the miRNAs highest confidence threshold (≥0.9) and disconnected nodes were

excluded to refine PPI network. Using Cytohubba tools[48], 10 highly scored genes that showed the shortest path according to degree were identified, **Figure 7B.** We identified 10 hub gene: ACTB**,** BCL2**,** CCND1**,** CDKN2A**,** ERBB2**(**also known as HER2**),** IL6**,** MYC**,** STAT3**,** TNF**,** TP53, all showed association and play critical role in BCa pathogenesis. TP53, MYC and ACTB are top central hub genes (red nodes), while genes like STAT3, BCL2 and CCND1 show moderate connectivity (orange nodes), CDKN2A, ERBB2, IL6 and TNF were still involved with fewer direct interactions (yellow nodes). The hub genes were reanalyzed in the STRING database using a high-confidence threshold (≥ 0.9) to ensure accurate and biologically relevant protein–protein interactions, to avoid false positive and weak interaction. The disconnected nodes were removed to identify core genes central to BCa progression **Figure 7C.** The chord diagram analysis **(Figure 8)** shows the regulatory interactions between dysregulated miRNAs (let-7c-5p, miR-99a-5p and miR-125b-5p) along with their target genes.Some miRNA regulates multiple target genes and several genes are controlled by more than one miRNA, which signify regulatory links within the network. The shared regulation shows a cooperative approach, where multiple miRNAs work together to manage gene expression more effectively. Cross-connections add redundancy to the system, which helps maintain stable gene expression even when individual regulatory pathways are disrupted. This network shows the complexity of post-transcriptional regulation and identifies key genes that play important roles in biological processes and BCa.

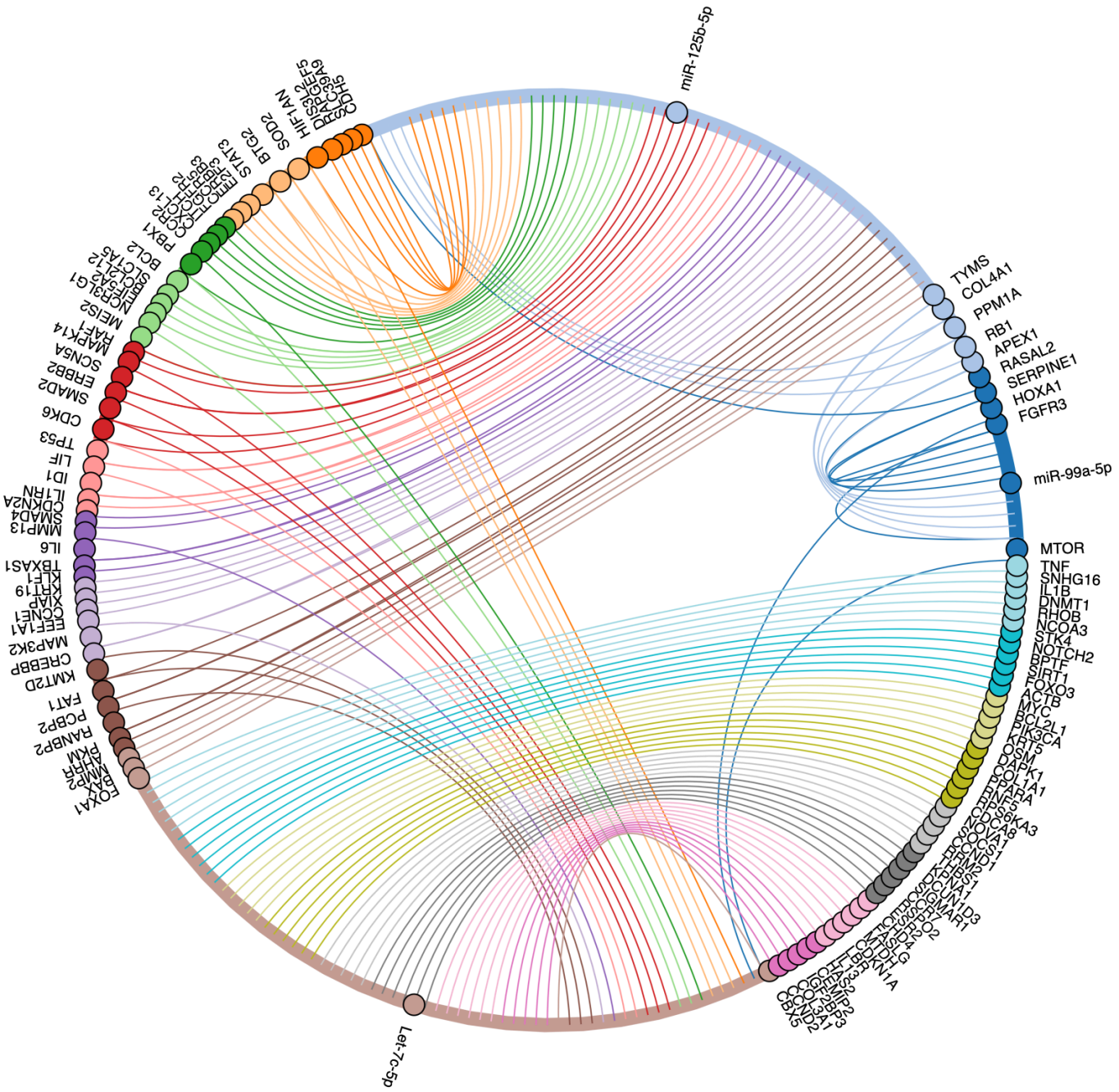
miR-125b-5p
miR-99a-5p
Let-7c-5p
TYMS
COL4A1
PPM1A
RB1
APEX1
RASAL2
SERPINE1
HOXA1
FGFR3
MTOR
TNF
SNHG16
IL1B
DNMT1
RHOB
NCOA3
STK4
NOTCH2
BPTF
SIRT1
FOXO3
ACTB
MYC
BCL2L1
PIK3CA
KRT5
OSM
DAPK1
COL1A1
PPP1R1A
NFKB1
PPP2CA
PPP2R5C
PPP2R5E
PPP2R5D
PPP2R5A
PPP2R2A
PPP2R2C
PPP2R2D
PPP2R2B
PPP2R2E
PPP2R2D
PPP2R2C
PPP2R2A

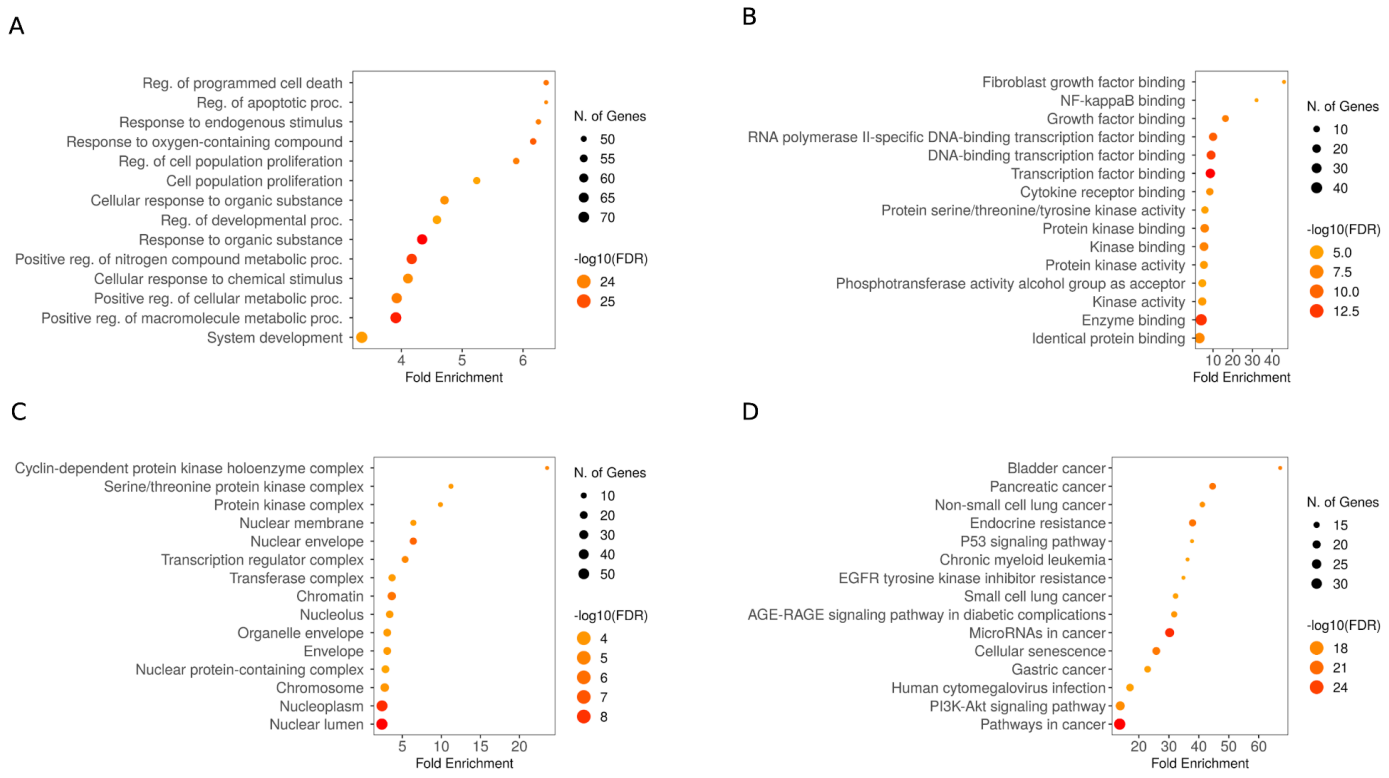

Figure 9: (A) Biological processes: illustrates metabolic pathways regulation essential for cellular processes and tumorigenesis, **(B)** Molecular function: shows crucial roles in transcription factor binding and kinase activity, **(C)** Cellular components: show significant roles in regulating gene expression and modulating cellular signaling, **(D)** KEGG pathway enrichment analysis: shows key cancer-related pathways emphasizing fold enrichment, significance, and gene involvement.

In biological process analysis **Figure 9 (A)**, the majority of genes are enriched in the response to endogenous stimuli and oxygen-containing compounds, apoptotic process regulation, programmed cell death regulation, and cell population proliferation regulation. Fibroblast growth factor binding, NF-kappaB binding, growth factor binding, and RNA polymerase II-specific DNA-binding transcription factor binding were all involved in the molecular function **Figure 9 (B)**. Cyclin-dependent protein kinase holoenzyme complex, serine/threonine protein kinase complex, protein kinase complex, nuclear membrane and envelope were the most abundant cellular components **Figure 9 (C)**. Using the KEGG database **Figure 9 (D)**, significant signaling pathways were identified,

indicating that candidate genes were mostly involved in P53 signaling, cancer pathways, non-small cell BCa,lung cancer, pancreatic cancer and endocrine resistance.

4. Discussion

This study demonstrates that urinary exosomal miRNAs from the let-7c cluster, particularly miR-99a-5p, can distinguish BCa patients from HC with high accuracy when analyzed using supervised ML. This is clinically relevant given the persistent challenge of differentiating BCa from benign urological conditions such as cystitis or urinary tract infection, which often present with overlapping symptoms like hematuria[49]. Current gold-standard diagnostic tools cystoscopy and urinary cytology remain invasive or insensitive, underscoring the need for reliable, non-invasive biomarkers. By showing that qRT-PCR derived miRNA data can be enhanced with ML to detect subtle expression changes, our findings contribute to efforts to translate molecular signatures into practical diagnostic tools.

Comparison with current diagnostic modalities

In routine clinical evaluation, patients with hematuria are assessed with urinalysis, imaging, cytology and cystoscopy[50]. Imaging modalities such as ultrasound and CT urography can identify larger or infiltrative tumors but lack resolution for flat or early-stage lesions and MRI is mainly used for staging rather than initial diagnosis[51]. Urine cytology, while highly specific (~78–86%), has poor sensitivity for LG tumors (~16%) and only moderate sensitivity for HG disease (~84%)[52]. Several FDA approved urine assays, including UroVysion FISH, ImmunoCyt/uCyt+ (Immunocytology test), NMP22 and BTA tests, have attempted to fill this gap but are limited by variable sensitivity and frequent false positives in benign conditions[53]. Our results suggest that exosomal miRNAs, when analyzed with ML, may overcome some of these limitations by offering biological specificity, resistance to degradation and the ability to capture subtle patterns not detectable with conventional approaches.

Expression patterns and diagnostic performance

We observed consistent downregulation of the let-7c-5p/miR-99a-5p/miR-125b-5p in BCa patients compared with HC, with miR-99a-5p emerging as the most robust diagnostic candidate across grade and stage analyses. Let-7c-5p and miR-125b-5p also showed downregulation, though less prominently, but may hold value in ratio-based features that reduce sample variability and capture biologically relevant interactions. Correlation analysis supported this view: in HC, miR-99a-5p and miR-125b-5p were strongly co-expressed, whereas let-7c-5p was largely independent, suggesting distinct regulatory mechanisms. These coordinated patterns were attenuated in cancer samples, consistent with disruption of normal regulatory interactions. Such findings highlight why ratio-based and multimodal features are advantageous in diagnostic modeling. In addition, the altered correlation patterns suggest a loss of coordinated regulation in the cancer state, highlighting potential changes in molecular interactions between healthy and malignant conditions.

Relation to prior studies

Our results both align with and diverge from prior studies. Spagnuolo et al. described significant upregulation of urinary let-7c in HG NMIBC, particularly T1 tumors, with strong stage-discrimination performance (AU-ROC= 0.80)[32]. While their study focused on prognostic risk stratification following BCG treatment in HG NMIBC, we observed downregulation of the Let-7c cluster in BCa across a broader clinical spectrum. Although stage-specific discrimination in our cohort was modest, these discrepancies may reflect differences in study design, cohort size or clinical context (prognostic vs diagnostic focus). Importantly, by integrating expression ratios and ML, we extended the clinical applicability of the cluster beyond prognostic stratification to diagnostic classification. Consistent with this, Zhang et al. demonstrated that urinary miR-99a and miR-125b are significantly downregulated in BCa, achieving AU-ROC values of 0.800 and 0.813, respectively, with a combined AU-ROC of 0.876, underscoring their diagnostic utility as non-invasive biomarkers[44]. In our study, miR-99a-5p emerged as the most consistent biomarker associated with disease presence, while let-7c-5p contributed more as a relatively low-expressing but stable biomarker within ratio-based

features. In contrast to its role as a primary classifier in previous prognostic approaches, let-7c-5p in our study serves a more refined purpose as a stable reference point within ratio features. This diverse functional role of let-7c-5p aligns with our earlier work, where we introduced our in-house algorithm for reference miRNA selection and identified let-7c-5p as a highly stable urinary exosomal miRNA across multiple urological conditions[54,55].

The downregulation of the let-7c cluster has been frequently observed in various cancer types, where its loss is commonly associated with tumor-suppressive functions and poor clinical outcomes[28,56–58]. Our findings are consistent with previous research, revealing that let-7c-5p is downregulated in BCa. However, its diagnostic ability was weaker to that of miR-99a-5p and miR-125b-5p, which were more effective at distinguishing BCa patients from HC. Previous studies have similarly reported reduced urinary expression of let-7c-5p in BCa, reinforcing its role as a tumor suppressor[59,60]. In contrast, Spagnuolo et al. 's findings of let-7c-5p upregulation in HG NMIBC further emphasize the context-dependent variability of its expression patterns[32]. miR-99a-5p emerged as the most reliable diagnostic marker in our study, a finding supported by multiple studies demonstrating its consistent downregulation in BCa tissues and urine[44,61–63]. Additionally, miR-125b-5p has been consistently reported as downregulated in BCa, strengthening its tumor-suppressive role[44,64–67].

ML integration

Logistic regression was chosen for its interpretability, robustness with small datasets and ability to generate probability estimates relevant to clinical decision-making. Bitin et al. employed a multi-modal approach, combining miRNA data with clinical variables and achieving an AU-ROC of 0.85. While their study utilized a broader set of miRNAs and clinical data, we demonstrated similar diagnostic accuracy (AU-ROC = 0.86, sensitivity 100%, accuracy 80%) and clear separation between BCa patients and HC with moderate grade classification through a more focused approach using qRT-PCR derived miRNA data and logistic regression. The inclusion of molecular and clinical variables improved diagnostic precision, though this may have been influenced by sample size and

class imbalance. The individual AU-ROC values of single miRNAs for stage discrimination were very low, further emphasizing the need for integrated models. These results should therefore be considered proof-of-concept rather than clinically validated. Further optimization using larger, balanced cohorts and more advanced algorithms such as ensemble or deep learning approaches may enhance performance, particularly for grade and stage classification.

Biological validation through bioinformatics

To ensure interpretability and biological relevance, we conducted integrative bioinformatics analyses. KEGG enrichment revealed associations of miR-99a-5p with PI3K–Akt, mTOR, and FGFR3 pathways, miR-125b-5p with p53, NF-κB, and HIF-1 signaling, and let-7c-5p with RAS/MAPK and cell cycle regulation. These pathways are central to BCa progression, underscoring the functional plausibility of our findings. PPI network analysis identified hub genes such as TP53, MYC, STAT3, EGFR, IGF1R and CCND1, reflecting the interplay of oncogenes and tumor suppressors in BCa biology. The coexistence of both stimulatory and inhibitory regulators illustrates why single miRNAs have limited discriminatory power, and why combined, ML-enabled signatures are needed to capture net biological effects. GO enrichment highlighted processes including DNA damage response, EMT, and immune modulation, further linking the cluster to key hallmarks of BCa. By directly regulating important oncogenic pathways like FGFR3 and mTOR, miR-99a-5p functions as a tumor suppressor biologically[68,69], thereby enhancing its biological significance and translational potential as a credible non-invasive biomarker. Collectively, these results imply that while urinary levels of the let-7c cluster may differ depending on tumor grade, disease stage or methodological considerations, our study's consistent downregulation, which is consistent with other reports, highlights the biological significance and diagnostic accuracy of this cluster in BCa.

Limitations and future directions

This study has several limitations. The single-center cohort was modest in size, limiting statistical power for grade- and stage-specific analyses and reducing generalizability. Validation in larger,

multi-center cohorts is required. The biomarker panel was restricted to three miRNAs and may not capture the full molecular complexity of BCa. Broader high-throughput profiling, coupled with functional validation, could refine biomarker panels and clarify mechanistic roles. Biological heterogeneity in urinary exosomes, which carry material from both malignant and non-malignant cells, also remains a challenge. Standardized protocols for exosome isolation, normalization, and qRT-PCR analysis will be essential for reproducibility across studies. From a modeling perspective, external validation is necessary to establish clinical robustness, and future work should test more advanced ML frameworks. Finally, our cross-sectional design precluded evaluation of prognostic utility; longitudinal studies are needed to determine whether these miRNAs can predict recurrence, progression, or treatment response. Integration with other modalities, such as mpMRI or VI-RADS, may further improve diagnostic precision and clinical adoption. At the same time, the biological heterogeneity of urinary exosomes carrying material from both malignant and non-malignant cells remains a challenge for reproducibility. Future studies should therefore focus on methods and tools to enrich tumor-derived exosomes. These results suggest that, when combined with ML techniques, urinary exosomal miRNA-based diagnostics offer a more precise and clinically applicable method for BCa detection and stratification. This approach could potentially reduce the need for invasive procedures while maintaining high sensitivity. Although this represents a significant advancement, the low AU-ROC emphasizes the need for further optimization. This could be achieved by adding more features to the model or adopting advanced model frameworks, such as ensemble methods or deep learning techniques, which could potentially enhance diagnostic accuracy.

5. Conclusion

This study provides proof of concept that urinary exosomal miRNAs, particularly miR-99a-5p, can contribute to BCa detection when analyzed within a ML framework. By integrating molecular and clinical features, our approach demonstrated reliable discrimination between BCa & HC and highlighted the value of ratio-based and multimodal features for diagnostic refinement. While current performance reflects the limitations of sample size and scope, these findings reinforce the promise of urinary exosomal miRNAs as non-invasive biomarkers and establish a foundation for larger validation

studies. Future efforts should focus on expanding biomarker panels, standardizing analytical pipelines and combining molecular signatures with imaging and clinical parameters to advance toward clinically deployable diagnostic tools.

6. Contributions

Research conceptualization and design: Kumar L, Jain G and Kural S; *Supervision and Validation*: Kumar L and Jain G; *Project Administration*: Kumar L; *Collection and/or assembly of data*: Kural S, Pathak AK, Singh S and Kumar L; *miRNAs analysis workflow*: Kural S; *Model Engineering/Development*: Pathak AK and Gupta M; *Data analysis and interpretation*: Pathak AK, Kural S, Singh S and Kumar L; *Visualization*: Kural S, Pathak AK and Singh S; *Writing- Original Draft*: Kural S, Pathak AK, Singh S, Jain G and Kumar L; *Resources*: Yadav M, Kumar U, Singh Y, Trivedi S and Das P; *Writing- Review & Editing*: Kumar L, Jain G, Gautam V, Gupta M, Das P, Kural S, Pathak AK and Singh S; *Funding Acquisition*: Kumar L

7. Funding

This research was supported by the *Institute of Eminence, Banaras Hindu University (BHU)* (Seed Grant to Kumar L and Seed Grant Research Fellowship to Kural S),

8. Conflict of interest

The authors declare that there are no conflicts of interest related to this work.

9. Informed Consent

Every participant received comprehensive information about the study and their participation was completely voluntary. Written consent was obtained before any data was collected.

10. Data Availability Statement

We are dedicated to promoting reproducibility and openness in research. Anonymous datasets and supplementary information used in this study can be shared for research or verification purposes, but access to patient-related data is limited to protect privacy and meet ethical standards. Subject to institutional approval and suitable data-sharing agreements, interested researchers can get in touch with the corresponding author and data will be made available upon reasonable request.

11. Acknowledgement

We would like to acknowledge the Centre for Genetic Disorders, Institute of Science, Banaras Hindu University (BHU) for providing essential laboratory facilities and research support throughout the course of this study. We are also grateful to the Department of Urology, Institute of Medical Sciences (IMS), BHU for their invaluable assistance in coordinating and facilitating sample collection. We also appreciate the support of the BioNEST, Central Discovery Centre, BHU for access to additional laboratory resources. We acknowledge the support of the Department of Computer Science, Institute of Science, BHU in developing and refining the ML models. We are sincerely thankful to all collaborators and the patients whose participation made this study possible.

12. Abbreviations

ACTB (Actin Beta)
AI (Artificial Intelligence)
AUC (Area under the curve)
AU-ROC (Area Under the Receiver Operating Characteristic)
BCa (Bladder Cancer)
BCG (Bacillus Calmette-Guérin)
BCSG (Bladder Cancer-Specific Genes)
BCL2 (B-cell Lymphoma 2)
BTA (Bladder Tumor Antigen)
CCND1 (Cyclin D1)
CDKN2A (Cyclin Dependent Kinase Inhibitor 2A)
cDNA (complementary DNA)
c-MYC (Cellular Myelocytomatosis Oncogene)
CT (Computed Tomography)
CTG (Common Target Genes)
Cytoscape (Network Visualization Software)

CytoHubba (Cytoscape plugin for hub gene analysis)
DMTF1 (Cyclin D Binding Myb-Like Transcription Factor 1)
EGFR (Epidermal Growth Factor Receptor)
EMT (Epithelial–Mesenchymal Transition)
ERBB2 / HER2 (Erb-B2 Receptor Tyrosine Kinase 2 / Human Epidermal Growth Factor Receptor 2)
EVs (Extracellular Vesicles)
FDA (U.S. Food and Drug Administration)
FGFR3 (Fibroblast Growth Factor Receptor 3)
FISH (Fluorescence In Situ Hybridization)
FPR (False Positive Rate)
GO (Gene Ontology)
HIF-1 (Hypoxia-Inducible Factor 1)
HMGA2 (High Mobility Group AT-Hook 2)
H-Ras (Harvey Rat Sarcoma Viral Oncogene Homolog)
IGF1R (Insulin-Like Growth Factor 1 Receptor)
IL6 (Interleukin 6)
KEGG (Kyoto Encyclopedia of Genes and Genomes)
LG (Low-Grade)
MAPK (Mitogen-Activated Protein Kinase)
miRNAs (microRNAs)
Mirbase (microRNA Database)
mirTarbase (microRNA–Target Interaction Database)
MIBCa (Muscle Invasive Bladder Cancer)
ML (Machine Learning)
MRI (Magnetic Resonance Imaging)
mTOR (Mammalian Target of Rapamycin)
MYC (MYC Proto-Oncogene)
NF-κB (Nuclear Factor kappa-light-chain-enhancer of activated B cells)
NMP22 (Nuclear Matrix Protein 22)
NMIBCa (Non–Muscle Invasive Bladder Cancer)
PDCD4 (Programmed Cell Death 4)
PI3K–Akt (Phosphoinositide 3-Kinase–Protein Kinase B signaling pathway)
PPI (Protein–Protein Interaction)
PTEN (Phosphatase and Tensin Homolog)
qRT-PCR (Quantitative Real-Time PCR)
RAS (Rat Sarcoma Viral Oncogene Homolog)
RNA Pol II (RNA Polymerase II)
ROC (Receiver Operating Characteristic)
STAT3 (Signal Transducer and Activator of Transcription 3)
TNF (Tumor Necrosis Factor)
TGP (Target Gene Panel)
TP53 (Tumor Protein P53)
TPR (True Positive Rate)
TURBT (Transurethral Resection of Bladder Tumor)
UTIs (Urinary Tract Infections)

13. Reference

1. Fang W, Yang ZY, Chen TY, Shen XF, Zhang C. Ethnicity and survival in bladder cancer: a population-based study based on the SEER database. *J Transl Med*. 2020;18(1):145. doi:10.1186/s12967-020-02308-w
2. Lobo N, Afferi L, Moschini M, et al. Epidemiology, Screening, and Prevention of Bladder Cancer. *Eur Urol Oncol*. 2022;5(6):628-639. doi:10.1016/j.euo.2022.10.003
3. Kumar L, Arya MC. Giant Vesical Calculus with Adenocarcinoma of the Bladder: A Rare Association. *J Endourol Case Rep*. 2020;6(2):83-85. doi:10.1089/cren.2019.0140
4. Shadab R, Nerli R, Bidi S, Ghagane S. Risk Factors for Bladder Cancer: Results of a Survey of Hospital Patients. *J Cancer Allied Spec*. 2022;9(1). doi:10.37029/jcas.v9i1.485
5. Jakus D, Šolić I, Jurić I, Borovac JA, Šitum M. The Impact of the Initial Clinical Presentation of Bladder Cancer on Histopathological and Morphological Tumor Characteristics. *J Clin Med*. 2023;12(13):4259. doi:10.3390/jcm12134259
6. Godlewski D, Bartusik-Aebisher D, Czech S, Szpara J, Aebisher D. Bladder cancer biomarkers. *Explor Target Anti-Tumor Ther*. 2025;6:1002301. doi:10.37349/etat.2025.1002301
7. Kural S, Pathak AK, Singh S, et al. Prospective Assessment of VI-RADS with Muscle Invasion in Urinary Bladder Cancer and Its Implication on Re-Resection/Restaging TURBT Patients. *Ann Surg Oncol*. 2025;32(1):609-618. doi:10.1245/s10434-024-16424-0
8. Gontero P, Birtle A, Capoun O, et al. European Association of Urology Guidelines on Non–muscle-invasive Bladder Cancer (TaT1 and Carcinoma In Situ)—A Summary of the 2024 Guidelines Update. *Eur Urol*. 2024;86(6):531-549. doi:10.1016/j.eururo.2024.07.027
9. Tripathy R, Kumar L, Agarwal S, et al. A Comparison Between Intravesical Gemcitabine Plus Docetaxel and Intravesical Bacillus Calmette-Guérin in the Treatment of Nonmuscle Invasive Naive Urinary Bladder Cancer: A Systematic Review and Meta-analysis of Oncological Outcomes. *Urology*. 2025;199:171-178. doi:10.1016/j.urology.2025.01.004
10. Kool R, Dragomir A, Kulkarni GS, et al. Benefit of Neoadjuvant Cisplatin-based Chemotherapy for Invasive Bladder Cancer Patients Treated with Radiation-based Therapy in a Real-world Setting: An Inverse Probability Treatment Weighted Analysis. *Eur Urol Oncol*. 2024;7(6):1350-1357. doi:10.1016/j.euo.2024.01.014
11. Bulai C, Geavlete P, Ene CV, et al. Detection of Urinary Molecular Marker Test in Urothelial Cell Carcinoma: A Review of Methods and Accuracy. *Diagn Basel Switz*. 2022;12(11):2696. doi:10.3390/diagnostics12112696
12. Singh S, Chen CC, Kim S, Singh A, Singh G. Role of Extracellular vesicle microRNAs and RNA binding proteins on glioblastoma dynamics and therapeutics development. *Extracell Vesicle*. 2024;4:100049. doi:10.1016/j.vesic.2024.100049
13. Aheget H, Mazini L, Martin F, Belqat B, Marchal JA, Benabdellah K. Exosomes: Their Role in Pathogenesis, Diagnosis and Treatment of Diseases. *Cancers*. 2020;13(1):84. doi:10.3390/cancers13010084
14. Felekkis K, Pieri M, Papaneophytou C. Exploring the Feasibility of Circulating miRNAs as Diagnostic and Prognostic Biomarkers in Osteoarthritis: Challenges and Opportunities. *Int J Mol Sci*. 2023;24(17):13144. doi:10.3390/ijms241713144
15. Li X, Yang L. Urinary exosomes: Emerging therapy delivery tools and biomarkers for urinary system diseases. *Biomed Pharmacother*. 2022;150:113055. doi:10.1016/j.biopha.2022.113055
16. Tripathy R, Kumar L, Kural S, Thakur A, Trivedi S, Sankhwar SN. The current status of miRNA in urinary bladder cancer: A minireview and strength, weakness, opportunity, and threat analysis. *Indian J Urol IJU J Urol Soc India*. 2025;41(2):98-103. doi:10.4103/iju.iju_442_24
17. Chattopadhaya A, Kural S, Verma A, et al. Urinary miRNAs in bladder cancer. *Clin Chim Acta*. 2025;567:120113. doi:10.1016/j.cca.2024.120113
18. O'Brien J, Hayder H, Zayed Y, Peng C. Overview of MicroRNA Biogenesis, Mechanisms of Actions, and Circulation. *Front Endocrinol*. 2018;9:402. doi:10.3389/fendo.2018.00402
19. Zhong X, Coukos G, Zhang L. miRNAs in human cancer. *Methods Mol Biol Clifton NJ*. 2012;822:295-306. doi:10.1007/978-1-61779-427-8_21
20. Gan L, Zheng L, Zou J, et al. MicroRNA-21 in urologic cancers: from molecular mechanisms to clinical implications. *Front Cell Dev Biol*. 2024;12:1437951. doi:10.3389/fcell.2024.1437951

21. Shen M, Chen T, Li X, et al. The role of miR-155 in urologic malignancies. *Biomed Pharmacother*. 2024;174:116412. doi:10.1016/j.biopha.2024.116412
22. Braicu C, Buiga R, Cojocneanu R, et al. Connecting the dots between different networks: miRNAs associated with bladder cancer risk and progression. *J Exp Clin Cancer Res*. 2019;38(1):433. doi:10.1186/s13046-019-1406-6
23. Chirshev E, Oberg KC, Ioffe YJ, Unternaehrer JJ. Let-7 as biomarker, prognostic indicator, and therapy for precision medicine in cancer. *Clin Transl Med*. 2019;8(1):24. doi:10.1186/s40169-019-0240-y
24. Yao Y, Zhang C, Xiong Y, Han B, Gao X, Wang S. [miR-let-7c-5p inhibits invasion and migration of bladder cancer cells by targeting HMGA2]. *Nan Fang Yi Ke Da Xue Xue Bao*. 2021;41(7):1022-1029. doi:10.12122/j.issn.1673-4254.2021.07.08
25. Vinall RL, Tepper CG, Ripoll AAZ, et al. Decreased expression of let-7c is associated with non-response of muscle-invasive bladder cancer patients to neoadjuvant chemotherapy. *Genes Cancer*. 2016;7(3-4):86-97. doi:10.18632/genesandcancer.103
26. Sun R, Wang C, Wang Y, et al. Role of miR-let-7c-5p/c-myc signaling axis in the committed differentiation of leukemic THP-1 cells into monocytes/macrophages. *Oncol Lett*. 2023;26(3):403. doi:10.3892/ol.2023.13989
27. Ma Y, Shen N, Wicha MS, Luo M. The Roles of the Let-7 Family of MicroRNAs in the Regulation of Cancer Stemness. *Cells*. 2021;10(9):2415. doi:10.3390/cells10092415
28. Truini A, Coco S, Nadal E, et al. Downregulation of miR-99a/let-7c/miR-125b miRNA cluster predicts clinical outcome in patients with unresected malignant pleural mesothelioma. *Oncotarget*. 2017;8(40):68627-68640. doi:10.18632/oncotarget.19800
29. Eniafe J, Jiang S. MicroRNA-99 family in cancer and immunity. *WIREs RNA*. 2021;12(3):e1635. doi:10.1002/wrna.1635
30. Wang Y, Huang D, Li M, Yang M. MicroRNA-99 family in cancer: molecular mechanisms for clinical applications. *PeerJ*. 2025;13:e19188. doi:10.7717/peerj.19188
31. Zhou H, Tang K, Xiao H, et al. A panel of eight-miRNA signature as a potential biomarker for predicting survival in bladder cancer. *J Exp Clin Cancer Res*. 2015;34(1):53. doi:10.1186/s13046-015-0167-0
32. Spagnuolo M, Costantini M, Ferriero M, et al. Urinary expression of let-7c cluster as non-invasive tool to assess the risk of disease progression in patients with high grade non-muscle invasive bladder Cancer: a pilot study. *J Exp Clin Cancer Res*. 2020;39(1):68. doi:10.1186/s13046-020-01550-w
33. Rahmani AM, Yousefpoor E, Yousefpoor MS, et al. Machine Learning (ML) in Medicine: Review, Applications, and Challenges. *Mathematics*. 2021;9(22):2970. doi:10.3390/math9222970
34. An Q, Rahman S, Zhou J, Kang JJ. A Comprehensive Review on Machine Learning in Healthcare Industry: Classification, Restrictions, Opportunities and Challenges. *Sensors*. 2023;23(9):4178. doi:10.3390/s23094178
35. Pathak AK, Dewangan BK, Gupta M. Predicting Cardiovascular Diseases Using Machine Learning. In: *Data Modelling and Analytics for the Internet of Medical Things*. 1st ed. CRC Press; 2023:109-125. doi:10.1201/9781003359951-9
36. Libbrecht MW, Noble WS. Machine learning applications in genetics and genomics. *Nat Rev Genet*. 2015;16(6):321-332. doi:10.1038/nrg3920
37. Kourou K, Exarchos TP, Exarchos KP, Karamouzis MV, Fotiadis DI. Machine learning applications in cancer prognosis and prediction. *Comput Struct Biotechnol J*. 2015;13:8-17. doi:10.1016/j.csbj.2014.11.005
38. Singh S, Pathak AK, Kural S, et al. Integrating miRNA profiling and machine learning for improved prostate cancer diagnosis. *Sci Rep*. 2025;15(1):30477. doi:10.1038/s41598-025-99754-7
39. Anandhi P, Nathiya DrE. Application of linear regression with their advantages, disadvantages, assumption and limitations. *Int J Stat Appl Math*. 2023;8(6):133-137. doi:10.22271/maths.2023.v8.i6b.1463
40. Ahsan MM, Luna SA, Siddique Z. Machine-Learning-Based Disease Diagnosis: A Comprehensive Review. *Healthc Basel Switz*. 2022;10(3):541. doi:10.3390/healthcare10030541
41. Huang S, Zhang X, Ni X, Chen L, Ruan F. Logistic regression analysis of the value of biomarkers, clinical symptoms, and imaging examinations in COVID-19 for SARS-CoV-2 nucleic acid detection. *Medicine (Baltimore)*. 2024;103(19):e38186. doi:10.1097/MD.0000000000038186
42. Tomiyama E, Fujita K, Hashimoto M, Uemura H, Nonomura N. Urinary markers for bladder cancer diagnosis: A review of current status and future challenges. *Int J Urol*. 2024;31(3):208-219. doi:10.1111/iju.15338
43. Kural S, Jain G, Agarwal S, Das P, Kumar L. Urinary extracellular vesicles-encapsulated miRNA signatures: A new paradigm for urinary bladder cancer diagnosis and classification. *Urol Oncol Semin Orig Investig*. 2024;42(7):179-190. doi:10.1016/j.urolonc.2024.03.006
44. Zhang DZ, Lau KM, Chan ESY, et al. Cell-Free Urinary MicroRNA-99a and MicroRNA-125b Are Diagnostic Markers for the Non-Invasive Screening of Bladder Cancer. Dahiya R, ed. *PLoS ONE*. 2014;9(7):e100793. doi:10.1371/journal.pone.0100793

45. Bitiņa-Barlote Ē, Bļizņuks D, Siliņa S, et al. Liquid Biopsy Based Bladder Cancer Diagnostic by Machine Learning. *Diagnostics*. 2025;15(4):492. doi:10.3390/diagnostics15040492
46. Cui S, Yu S, Huang HY, et al. miRTarBase 2025: updates to the collection of experimentally validated microRNA–target interactions. *Nucleic Acids Res*. 2025;53(D1):D147-D156. doi:10.1093/nar/gkae1072
47. Griffiths-Jones S. miRBase: microRNA sequences, targets and gene nomenclature. *Nucleic Acids Res*. 2006;34(90001):D140-D144. doi:10.1093/nar/gkj112
48. Chin CH, Chen SH, Wu HH, Ho CW, Ko MT, Lin CY. cytoHubba: identifying hub objects and sub-networks from complex interactome. *BMC Syst Biol*. 2014;8(S4):S11. doi:10.1186/1752-0509-8-S4-S11
49. Shih DH, Shih PL, Wu TW, Lee CX, Shih MH. Distinguishing Bladder Cancer from Cystitis Patients Using Deep Learning. *Mathematics*. 2023;11(19):4118. doi:10.3390/math11194118
50. Buteau A, Seideman CA, Svatek RS, et al. What is evaluation of hematuria by primary care physicians? Use of electronic medical records to assess practice patterns with intermediate follow-up. *Urol Oncol Semin Orig Investig*. 2014;32(2):128-134. doi:10.1016/j.urolonc.2012.07.001
51. Galgano SJ, Porter KK, Burgan C, Rais-Bahrami S. The Role of Imaging in Bladder Cancer Diagnosis and Staging. *Diagn Basel Switz*. 2020;10(9):703. doi:10.3390/diagnostics10090703
52. Yafi FA, Brimo F, Steinberg J, Aprikian AG, Tanguay S, Kassouf W. Prospective analysis of sensitivity and specificity of urinary cytology and other urinary biomarkers for bladder cancer. *Urol Oncol Semin Orig Investig*. 2015;33(2):66.e25-66.e31. doi:10.1016/j.urolonc.2014.06.008
53. Wan X, Wang D, Zhang X, et al. Unleashing the power of urine‐based biomarkers in diagnosis, prognosis and monitoring of bladder cancer (Review). *Int J Oncol*. 2025;66(3):18. doi:10.3892/ijo.2025.5724
54. Pathak AK, Kural S, Singh S, et al. Development of a robust and generalizable algorithm "gQuant" for accurate normalizer gene selection in qRT-PCR analysis. *Sci Rep*. 2024;14(1):18774. doi:10.1038/s41598-024-66770-y
55. Pathak A, Kural S, Singh S, Kumar L, Gupta M, Jain G. Analysis of qRT-PCR Data to Identify the Most Stable Reference Gene Using gQuant. *BIO-Protoc*. 2025;15(1370). doi:10.21769/BioProtoc.5292
56. Bailey ST, Westerling T, Brown M. Loss of Estrogen-Regulated microRNA Expression Increases HER2 Signaling and Is Prognostic of Poor Outcome in Luminal Breast Cancer. *Cancer Res*. 2015;75(2):436-445. doi:10.1158/0008-5472.CAN-14-1041
57. Cappuzzo F, Sacconi A, Landi L, et al. MicroRNA Signature in Metastatic Colorectal Cancer Patients Treated With Anti-EGFR Monoclonal Antibodies. *Clin Colorectal Cancer*. 2014;13(1):37-45.e4. doi:10.1016/j.clcc.2013.11.006
58. Lin KY, Ye H, Han BW, et al. Genome-wide screen identified let-7c/miR-99a/miR-125b regulating tumor progression and stem-like properties in cholangiocarcinoma. *Oncogene*. 2016;35(26):3376-3386. doi:10.1038/onc.2015.396
59. Hofbauer SL, De Martino M, Lucca I, et al. A urinary microRNA (miR) signature for diagnosis of bladder cancer. *Urol Oncol Semin Orig Investig*. 2018;36(12):531.e1-531.e8. doi:10.1016/j.urolonc.2018.09.006
60. Pardini B, Cordero F, Naccarati A, et al. microRNA profiles in urine by next-generation sequencing can stratify bladder cancer subtypes. *Oncotarget*. 2018;9(29):20658-20669. doi:10.18632/oncotarget.25057
61. Borkowska EM, Kutwin P, Rolecka D, Konecki T, Borowiec M, Jabłonowski Z. Clinical value of microRNA-19a-3p and microRNA-99a-5p in bladder cancer. *Arch Med Sci AMS*. 2023;19(3):694-702. doi:10.5114/aoms.2019.89700
62. Feng Y, Kang Y, He Y, et al. microRNA-99a acts as a tumor suppressor and is down-regulated in bladder cancer. *BMC Urol*. 2014;14(1):50. doi:10.1186/1471-2490-14-50
63. Liu Y, Li B, Yang X, Zhang C. MiR‐99a‐5p inhibits bladder cancer cell proliferation by directly targeting mammalian target of rapamycin and predicts patient survival. *J Cell Biochem*. 2019;120(12):19330-19337. doi:10.1002/jcb.27318
64. Huang L, Luo J, Cai Q, et al. MicroRNA‐125b suppresses the development of bladder cancer by targeting E2F3. *Int J Cancer*. 2011;128(8):1758-1769. doi:10.1002/ijc.25509
65. Avellini C, Licini C, Lazzarini R, et al. The trophoblast cell surface antigen 2 and miR-125b axis in urothelial bladder cancer. *Oncotarget*. 2017;8(35):58642-58653. doi:10.18632/oncotarget.17407
66. Zhao X, He W, Li J, et al. MiRNA-125b inhibits proliferation and migration by targeting SphK1 in bladder cancer. *Am J Transl Res*. 2015;7(11):2346-2354.
67. Liu S, Chen Q, Wang Y. MiR-125b-5p suppresses the bladder cancer progression via targeting HK2 and suppressing PI3K/AKT pathway. *Hum Cell*. 2020;33(1):185-194. doi:10.1007/s13577-019-00285-x
68. Wu D, Zhou Y, Pan H, Zhou J, Fan Y, Qu P. microRNA-99a inhibiting cell proliferation, migration and invasion by targeting fibroblast growth factor receptor 3 in bladder cancer. *Oncol Lett*. 2014;7(4):1219-1224. doi:10.3892/ol.2014.1875
69. Drayton RM, Peter S, Myers K, et al. MicroRNA-99a and 100 mediated upregulation of FOXA1 in bladder cancer. *Oncotarget*. 2014;5(15):6375-6386. doi:10.18632/oncotarget.2221